

# Tailoring dual-phase steel properties through controlled temperature and holding time during heat treatment

Emmanuel Olorundaisi<sup>1\*</sup>, and Peter A. Olubambi<sup>1</sup>

<sup>1</sup>Centre for Nanoengineering and Advanced Materials, School of Mining, Metallurgy and Chemical Engineering, University of Johannesburg, Johannesburg 2092, South Africa.

**Abstract.** This study investigates the effect of controlled temperature and holding time on the microstructure and properties of DP600 dual-phase steel. Low-carbon steel (0.3 wt%C) was heat-treated at 850°C with holding times of 20, 40, 60, and 80 minutes, followed by quenching in bitumen. The microstructure revealed variations in ferrite-martensite dispersion with increasing holding time. Improved mechanical properties were observed due to microstructural evolution, while corrosion resistance decreased with prolonged exposure. The findings highlight the critical role of heat treatment parameters in optimizing dual-phase steel properties for engineering applications.

## 1 Introduction

Dual-phase (DP) steels represent a class of advanced high-strength steels (AHSS) extensively utilized in automotive, structural, and industrial sectors due to their superior balance of strength, ductility, and toughness. The typical microstructure comprises a ductile ferritic matrix reinforced by a hard martensitic phase, which synergistically enhances mechanical performance [1]. This dual-phase configuration offers advantages over conventional steels, including improved weldability and formability, making DP steels highly desirable in manufacturing applications [2,3].

The development of DP steels is fundamentally governed by alloy chemistry and thermo-mechanical processing conditions, particularly heat treatment parameters such as intercritical annealing temperature, holding time, cooling rate, and the choice of quenching medium. These factors collectively influence phase transformation kinetics, grain refinement, and the resultant ferrite–martensite morphology, all of which are critical to tailoring mechanical and corrosion properties [2,4–6].

Intercritical annealing, a standard heat treatment process for DP steels, involves heating within the dual-phase (ferrite + austenite) region followed by rapid quenching. The austenite formed during heating transforms into martensite upon quenching, while ferrite remains unaltered [1,7]. The temperature and duration of annealing critically affect the extent of austenite formation and carbon redistribution, which in turn determine the volume fraction and distribution of martensite. Prolonged holding times enhance carbon diffusion, leading to higher martensite content and, consequently, increased hardness and tensile strength [8].

However, excessive thermal exposure may also alter corrosion behaviour, making optimization essential.

The morphology and dispersion of martensite within the ferrite matrix significantly impact mechanical properties. A uniform, isolated distribution of martensite within the ferrite yields higher strength and better strain distribution compared to a network/chain-like martensite arrangement, which may act as a site for crack initiation [9,10]. Furthermore, martensite volume fraction can be precisely controlled through thermal cycles, offering a pathway to fine-tune the strength–ductility trade-off.

Several studies have emphasized the importance of heat treatment parameters in developing optimal DP microstructures. For instance, Caballero et al. (2006) [11] highlighted the effect of cooling rate and soaking time at low intercritical temperatures on microstructural refinement. Similarly, Panda et al. (2000) [12] observed enhanced ferrite formation through controlled intercritical annealing followed by quenching. Alaneme and Kamma (2010) [13] demonstrated that appropriate selection of treatment conditions could produce duplex microstructures with favourable mechanical responses.

Beyond mechanical performance, corrosion resistance is increasingly recognized as a critical property of DP steels, especially for structural applications exposed to aggressive environments [14]. The martensite-rich regions are more prone to electrochemical degradation due to their higher dislocation density and carbon content. Salamci et al. (2017) [15] reported that increasing the martensite volume fraction correlates with higher corrosion rates, highlighting the need for a balanced microstructure to ensure longevity and environmental compatibility.

This study investigates DP600 steel, a low-carbon variant containing 0.3 wt% C, subjected to intercritical annealing at 850°C for varying holding times (20, 40, 60, and 80 minutes), followed by quenching in bitumen [7,16–19]. The unconventional use of bitumen as a quenching medium introduces a unique cooling profile, potentially beneficial for microstructural control [20]. Bitumen offers several advantages, including low thermal conductivity, water insolubility, chemical inertness, and good thermal stability, which can moderate heat extraction and influence transformation behaviour [21]. Its economic viability and environmental compatibility further justify its selection for experimental exploration. The primary objective of this research is to elucidate the influence of intercritical annealing temperature and holding time on the microstructural evolution and associated property changes in DP600 steel. Specifically, the study examines variations in density, tensile and yield strengths, hardness, and corrosion resistance. By correlating thermal treatment conditions with performance metrics, this work provides insights into optimizing DP steel processing for targeted engineering applications requiring high strength, adequate ductility, and enhanced corrosion resistance.

## 2 Methodology

Table 1 shows the chemical composition of the as-received DP600 steel. The sample was sectioned using wire electrical discharge machining (EDM) into five specimens with dimensions of 2 × 10 mm. Four specimens were subjected to heat treatment at an intercritical annealing temperature of 850 °C for varying holding times of 20, 40, 60, and 80 minutes, while the fifth specimen served as the control and was not heat-treated. Following annealing, the heat-treated specimens were rapidly quenched in bitumen (SS 60–70 grade) maintained at 230 °C for 10 minutes, then allowed to air-cool to room temperature. This quenching process facilitated the transformation of austenite to martensite and minimized retained austenite and residual stresses. Quenching in bitumen influences the transformation of austenite to martensite in a way that balances cooling severity and uniformity, which is particularly important for low-carbon steels. Unlike water or brine, which quench too rapidly

and cause steep thermal gradients, bitumen cools the steel more gradually due to its higher viscosity and lower thermal conductivity. This moderated cooling rate is still sufficient to suppress the diffusion-controlled transformations of austenite to pearlite or bainite, thereby allowing a portion of the austenite to transform into martensite.

Before microstructural examination was done, the prepared samples were hot-mounted with a Struers CitoPress-1 Machine. Proceeded by grinding and polishing of the sample's face thoroughly, using Struers TegraPol-11 550 Machine, with disc grades of 90, 220, and 330 in succession. The samples were washed and air-dried, followed by etching with a 3% nital solution. The surface microstructure was examined with a JEOL JSM-7900F SEM. The microstructural behaviour was examined using SEM images. Additionally, to evaluate the XRD of the heat-treated sample, the Panalytical X'Pert Pro diffractometer was used. It has a Cu-K source with a 40 kV and 20 mA voltage that operates over a 5–90-degree angle range at 1.5406 wavelength. The micro-hardness was determined using the Vickers indentation method at an applied load of 500gf with a time of 15s. On the sample, five indentations were made; the hardness was determined by averaging them.

Subsequent to heat treatment, all samples underwent standard metallographic preparation for microstructural evaluation and further characterization. Corrosion behaviour was assessed using the linear potentiodynamic polarization technique. The analysis was conducted in a 0.5 M H<sub>2</sub>SO<sub>4</sub> solution, employing a three-electrode electrochemical cell system. The working electrode was the DP steel sample, while a platinum counter electrode and a saturated calomel reference electrode (SCE) completed the setup. The electrochemical tests were performed at a potential range of -1.5 V to +1.5 V, with a scan rate of 0.0015 V/s and a constant current range between 10 nA and 10 mA for 600 seconds (10 minutes). Corrosion parameters such as corrosion rate (mm/year), corrosion potential (V), polarization resistance ( $\Omega$ ), and corrosion current density (A/cm<sup>2</sup>) were measured to evaluate the anti-corrosion performance of the developed DP steel.

**Table 1.** Chemical analysis of the low carbon steel.

Elements	Fe	C	Mn	Si	Al	B	Nb	Cr	Cu	Ni	S	P
<b>Composition (wt%)</b>	94.168	0.13	2.03	1.0	0.92	0.004	0.14	1.3	0.2	0.048	0.01	0.05

## 3 Results

### 3.1 Mechanical analysis

The mechanical properties of the normalized (as-received) sample show a bulk hardness of 89.45 HV. This value reflects the predominance of ferrite in the microstructure, with minimal martensitic contribution due to the absence of heat treatment. In contrast, the heat-treated samples exhibited a significant increase in hardness with prolonged holding times at the intercritical annealing temperature of 850 °C. The Vickers hardness values rose progressively from 203.15 HV (20 min) to 224.45 HV (80 min), indicating a strong correlation between holding time and microstructural transformation as reported in our earlier findings [22].

This consistent increase in hardness is attributed primarily to the enhanced formation of martensite. As the holding time increases, a greater volume of austenite is stabilized due to extended diffusion of carbon at the intercritical temperature [23]. During quenching, this austenite transforms into hard, brittle martensite, contributing to the observed hardness improvement. Notably, the hardness increment between 60 minutes (223.75 HV) and 80

minutes (224.45 HV) is marginal, suggesting that the material approaches a saturation point in martensite formation. This plateau effect implies that further extension of holding time yields diminishing returns, potentially due to the full transformation of available austenite and near-complete carbon redistribution. The initially lower hardness at 20 minutes may result from insufficient austenite formation or retained residual stresses from quenching. At shorter durations, the austenite fraction may be inadequate to form a high percentage of martensite upon cooling, leading to a lower hardness compared to samples held for longer times [24,25].

Furthermore, the rise in strength can also be linked to secondary hardening effects, such as the possible precipitation of fine carbide phases during quenching or tempering. These carbides may originate from supersaturated carbon in body-centered tetragonal martensite, contributing to dispersion strengthening [12]. It could be concluded that the intercritical annealing at 850 °C followed by bitumen quenching significantly enhances the hardness and strength of DP600 steel. However, an optimal holding time of around 60 minutes may offer the best trade-off between property enhancement and process efficiency, as prolonged soaking beyond this point introduces minimal improvement and may risk adverse effects such as grain coarsening or carbide overgrowth.

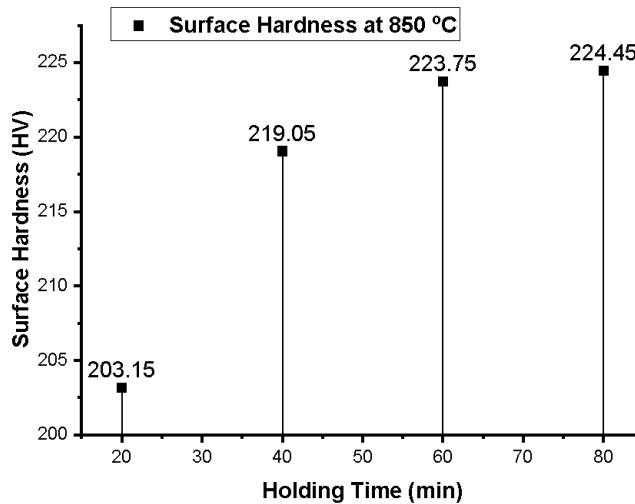
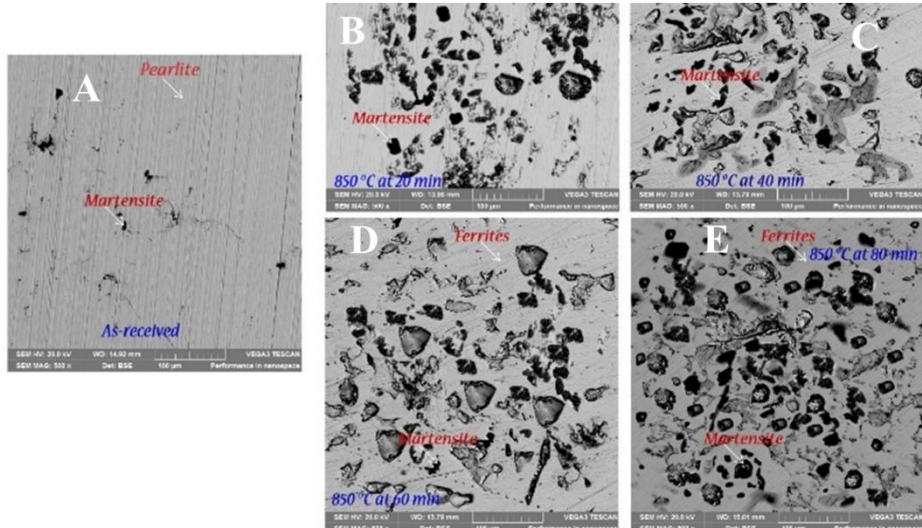


**Fig. 1.** SH of the heat-treated sample at 850 °C at different HT.

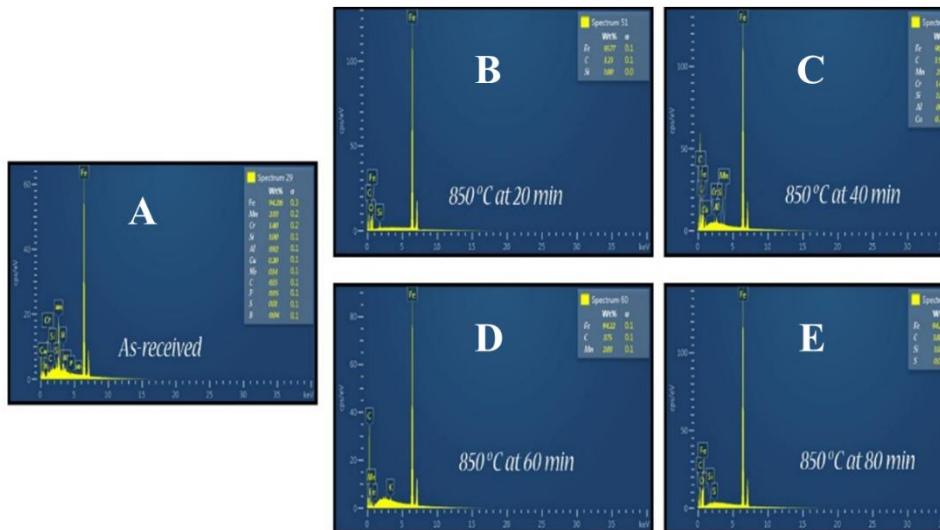
### 3.2 Microstructural and compositional analysis

Figure 2 illustrates the microstructural evolution of DP steel subjected to intercritical annealing at 850 °C for varying holding times, 20, 40, 60, and 80 minutes, as well as that of the as-received (normalized) sample. In the as-received condition, the microstructure is characteristic of hypo-eutectoid steel, comprising a large fraction of ferrite with sparse pearlite regions. This ferrite-dominant matrix explains the comparatively lower hardness and strength of the untreated sample. Upon intercritical annealing and subsequent quenching in bitumen, significant microstructural transformation is observed. The dark regions in the micrographs represent martensite, while the lighter, greyish background indicates the ferrite matrix. As the holding time increases, a larger fraction of austenite is stabilized during annealing, which subsequently transforms into martensite upon quenching. The increased martensitic fraction with longer holding durations corresponds to the elevated hardness values previously discussed. Notably, the martensite appears in a chain-like or networked

distribution within the ferrite matrix. Such morphology enhances mechanical interlocking and impedes dislocation motion, thereby improving hardenability and strength. The microstructural refinement and phase distribution directly influence the material's mechanical performance, making the heat-treated samples significantly harder than the as-received steel.



**Fig. 2.** Microstructure of the heat-treated sample at 850 °C at different holding time: (A) As received, (B) for 20 min, (C) for 40 min, (D) for 60 min, and (E) for 80 min.



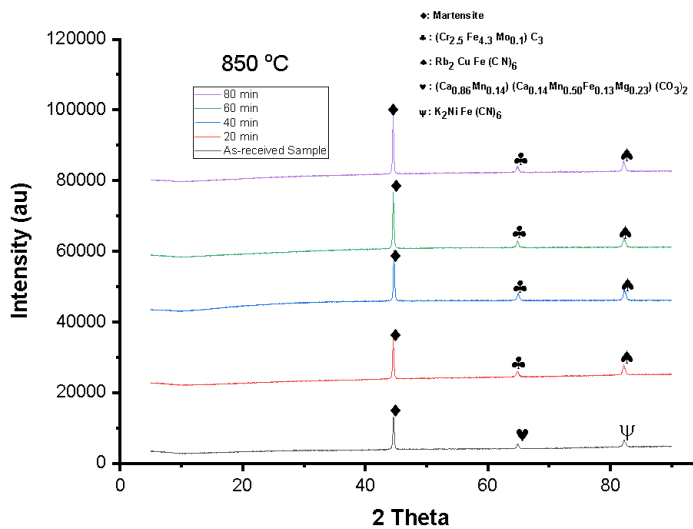
**Fig. 3.** EDS spectra of the heat-treated sample at 850 °C at different holding time: (A) As received, (B) for 20 min, (C) for 40 min, (D) for 60 min, and (E) for 80 min.

Figure 3 presents the Energy-Dispersive X-ray Spectroscopy (EDS) spectra of both the as-received and heat-treated samples. The EDS results for the as-received steel confirm its low-carbon composition, with carbon content at approximately 0.13% and iron constituting about 94.216% by weight. In contrast, the EDS spectra of the heat-treated samples reveal a gradual increase in carbon content with increasing holding time. This apparent carbon

enrichment may be attributed to carbon absorption or surface retention effects from the bitumen quenching medium. Bitumen, being a hydrocarbon-based material, could potentially deposit carbonaceous residues during rapid cooling, influencing the localized surface composition. In summary, the microstructural changes induced by intercritical annealing and bitumen quenching not only enhance the mechanical properties of DP steel through increased martensite formation but also suggest compositional modifications, possibly due to the interaction with the quenching medium. These findings underscore the importance of controlling both thermal treatment parameters and quenching environments in tailoring the microstructure and performance of advanced high-strength steels.

### 3.3 X-ray diffraction (XRD) analysis

Figure 4 displays the XRD patterns of the as-received DP steel and the heat-treated samples annealed at 850 °C for varying holding times. The as-received sample exhibits a prominent diffraction peak at a  $2\theta$  angle of  $44.5^\circ$ , with an intensity of 13,218.24 arbitrary units (a.u.), corresponding to the presence of a carbon-rich iron phase ( $\text{Co}_{0.055}\text{Fe}_{1.945}$ ), which is indicative of a BCC crystal structure. This confirms the ferritic nature of the steel in its normalized condition. Additional diffraction peaks at  $2\theta$  angles of  $64.9^\circ$  and  $82.2^\circ$ , with intensities of 5512.17 a.u. and 6724.39 a.u., respectively, indicate the presence of secondary phases such as calcium manganese iron magnesium carbonate ( $(\text{Ca}_{0.86}\text{Mn}_{0.14})(\text{Ca}_{0.14}\text{Mn}_{0.50}\text{Fe}_{0.13}\text{Mg}_{0.23})(\text{CO}_3)_2$ ) and potassium nickel iron cyanide ( $\text{K}_2\text{NiFe}(\text{CN})_6$ ). These may originate from minor impurities, prior surface treatments, or interactions with the quenching environment.



**Fig. 4.** XRD of the heat-treated sample at 850 °C at different HT.

Upon heat treatment at 850 °C and subsequent quenching in bitumen, significant phase transformations are observed. The XRD patterns of the heat-treated samples reveal an increase in the intensity and sharpness of martensitic peaks, indicating the formation of a greater volume fraction of martensite. This is attributed to the stabilization of austenite during intercritical annealing and its transformation into martensite upon quenching. The presence of bitumen as a quenching medium may have further contributed to localized carbon enrichment, enhancing the formation of martensite. Notably, the martensitic peak intensity increases progressively with holding time, as shown in Table 2, suggesting that longer

exposure at the intercritical temperature promotes greater austenite formation, which upon quenching transforms into martensite. The growth in peak height with holding time also correlates well with the earlier observed trend in hardness and mechanical strength, reinforcing the microstructure–property relationship.

In summary, the XRD analysis confirms the transformation from a primarily ferritic structure in the as-received sample to a ferrite–martensite dual-phase structure in the heat-treated specimens. The increasing peak intensity of martensite with prolonged holding time highlights the influence of thermal exposure and quenching medium on phase evolution and material performance.

**Table 2.** Peak height of DP steel heated at intercritical annealing temperature of 850 °C.

Holding Time	Peak height
20 min	18733.05
40 min	20428.37
60 min	23912.48
80 min	25314.13
As-received	13218.24

The crystallite grain size of the sample was calculated using equation 1 below:

$$D = \frac{K\lambda}{\beta \cos\theta} \quad (1)$$

Where:

D is the crystallites size

K is the Scherrer constant given as 0.9

$\lambda$  is the wavelength of the X-ray used, given as 0.154060  $\mu\text{m}$

$\beta$  is the FWHM (Full width at half of the maximum) in radians.

$\theta$  is the peak position in radians

The degree of crystallinity of the sample is calculated as thus from equation 2:

$$\text{Crystallinity (\%)} = \frac{\text{Area of crystalline peak}}{\text{Area of all peaks}} * 100 \quad (2)$$

Crystallite size plays a significant role in determining the physical and mechanical behaviour of DP steels. Generally, a reduction in crystallite size enhances mechanical performance, particularly strength and hardness, due to the grain boundary strengthening mechanism, also known as the Hall-Petch effect. Fine crystallites act as barriers to dislocation motion, thereby increasing the material's resistance to plastic deformation. The degree of crystallinity, which reflects the extent of ordered atomic arrangement within the material, is strongly influenced by both the chemical composition and the thermal history, especially cooling rates and annealing conditions. A higher degree of crystallinity typically results in increased stiffness and strength but may also lead to a reduction in ductility, making the material more brittle.

According to Table 3, as the HT at 850 °C increases, the crystallite size consistently decreases, while the degree of crystallinity increases. This indicates that extended thermal exposure allows for more complete phase transformation and structural ordering. The reduction in crystallite size, combined with increased crystallinity, contributes to improved strength and hardness, as observed in the sample quenched after 80 minutes. Therefore, the superior mechanical properties of DP steel annealed at 850 °C and held for 80 minutes can be attributed to this optimal combination of fine crystallite structure and high crystallinity. These microstructural characteristics enhance dislocation resistance and phase stability, reinforcing the material's performance under mechanical loading.

**Table 3.** Crystallinity properties of DP steel at 850 °C T.

HT (min)	Peak Position(2θ)	FWHM (β)	Crystallite Size D (nm)	Average D (nm)	Average D (μm)	Crystalline (%)
20	44.5569	0.2397	93.0326			
	64.8719	0.5442	68.7533	119.7653	0.1198	71.44
	82.2119	0.5936	197.5099			
40	44.5909	0.2466	90.4638			
	64.9229	0.5724	65.4927	119.3658	0.1194	81.55
	82.2629	0.5838	202.1409			
60	44.5229	0.2290	97.3018			
	64.7869	0.6036	61.7941	118.5776	0.1186	87.77
	82.1609	0.5924	196.6370			
80	44.5399	0.2324	95.9189			
	64.8039	0.6383	58.4688	114.7488	0.1147	91.44
	82.1609	0.6136	189.8589			
As-Received	44.6589	0.2330	95.8886			
	64.9569	0.4271	87.8936	143.8270	0.1438	19.45
	82.2799	0.4775	247.6989			

### 3.4 Corrosion behaviour of as-received and heat-treated DP steel

Figure 5 illustrates the polarization curves of the as-received and heat-treated low-carbon DP steels, obtained via Tafel extrapolation in a 0.5 M H<sub>2</sub>SO<sub>4</sub> acidic environment. The anodic and cathodic branches of the polarization curves were used to determine key electrochemical

parameters: corrosion current density ( $j_{corr}$ ), corrosion rate (mm/year), corrosion potential ( $E_{corr}$ ), and polarization resistance ( $R_p$ ), with a summary presented in Table 4. The as-received sample exhibited the highest corrosion rate of 3.1121 mm/year, which is indicative of poor corrosion resistance. This behavior is attributed to the formation of a thin, unstable oxide layer on the ferrite-rich surface, offering minimal protective effect. The corrosion potential ( $E_{corr}$ ) was measured at  $-0.46$  V, with a relatively high corrosion current density of  $2.44 \times 10^{-4}$  A/cm<sup>2</sup>, and a low polarization resistance of 84.193  $\Omega$ , suggesting rapid electrochemical degradation. For the heat-treated samples, the corrosion rate increased progressively with holding time. This trend is consistent with the increasing volume fraction of martensite, which is known to accelerate localized galvanic interactions between martensitic and ferritic regions, thus enhancing corrosion susceptibility. As previously reported by Salamci et al. (2017) [15], the presence of martensite, with its higher dislocation density and residual stress, acts as an anodic site, thereby facilitating corrosion in acidic media.

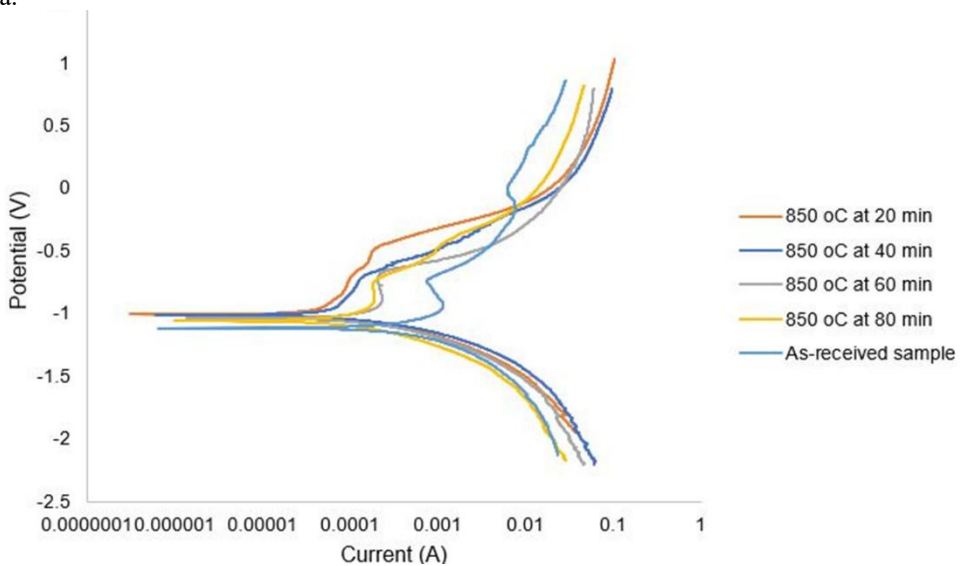


**Fig. 5.** Polarization curves of the heat-treated sample at 850 °C at different HT

**Table 4.** Tafel extrapolation outcome of DP steel at 850 °C at different HT.

Specimen	Corrosion Potential (V)	Corrosion Density (A/cm <sup>2</sup> )	Polarization resistance ( $\Omega$ )	Corrosion rate (mm/year)
As-received Sample	-1.1172	$2.44 \times 10^{-4}$	84.193	3.1121
850 °C @ 20 min.	-1.0224	$2.68 \times 10^{-4}$	422.02	1.9036
850 °C @ 40 min	-1.0352	$1.72 \times 10^{-4}$	287	1.9377
850 °C @ 60 min	-1.0476	$7.97 \times 10^{-5}$	245.45	2.0004
850 °C @ 80 min	-1.119	$2.40 \times 10^{-5}$	129.61	2.8325

The sample heat-treated at 850 °C and held for 80 minutes exhibited the highest corrosion rate among the heat-treated conditions, with a value of 2.833 mm/year, a corrosion potential of  $-1.12$  V, a corrosion current density of  $2.40 \times 10^{-5}$  A/cm<sup>2</sup>, and a relatively low polarization resistance of 129.61 Ω. Although this rate is slightly lower than the as-received steel, it still indicates significant susceptibility due to the elevated martensite content. Figure 5 further illustrates the progressive shift of the polarization curves toward the more noble (positive) direction, signifying the electrochemical adjustment of the DP steel system as the microstructure evolves through increased martensitic transformation. This shift correlates with structural changes and altered surface reactivity due to phase morphology and distribution. In summary, while heat treatment enhances mechanical strength via martensitic transformation, it simultaneously reduces corrosion resistance, particularly at prolonged holding times, due to the electrochemical activity associated with martensitic phases.

## Conclusion

This study examined the effect of intercritical annealing at 850 °C for varying holding times (20, 40, 60, and 80 minutes) followed by quenching in bitumen on the microstructure, mechanical properties, crystallographic features, and corrosion behavior of low-carbon DP steel. The results demonstrated that increasing the holding time led to a progressive transformation of austenite to martensite, which significantly enhanced the hardness and strength of the material. The Vickers hardness values increased steadily with holding time, reaching a peak at 80 minutes due to the higher volume fraction and uniform distribution of martensite within the ferrite matrix. XRD analysis confirmed a shift in phase composition with increasing martensitic intensity, and a decrease in crystallite size coupled with an increase in the degree of crystallinity, both contributing to improved mechanical performance. Microstructural observations revealed a clear transition from a ferrite-pearlite structure in the as-received steel to a ferrite–martensite dual-phase structure in heat-treated samples. The martensite appeared in a chain-like configuration within the ferrite matrix, enhancing mechanical interlocking and hardenability. However, an inverse relationship was observed between mechanical strength and corrosion resistance. The corrosion rate increased with holding time, with the sample held for 80 minutes showing the highest susceptibility to corrosion, attributed to the elevated martensite content. The electrochemical data indicated a shift in corrosion potential and a decrease in polarization resistance, consistent with increased electrochemical activity of martensitic regions. In conclusion, while extended intercritical annealing and bitumen quenching significantly enhance the mechanical properties of DP steel, they also increase its corrosion vulnerability. Therefore, a balance between mechanical performance and corrosion resistance must be carefully considered, with an optimal holding time around 60 minutes, offering the best compromise between strength and durability for structural applications.

There is no special grant for this research. However, necessary support was given by the Department of Metallurgical Engineering of University of Johannesburg, Johannesburg, South Africa.

Data availability: The data used in this research are not available publicly. However, it can be obtained from the authors once a justifiable request is made.

## References

- [1] Z. Li, D. Wu, W. Lü, H. Yu, Z. Shao, L. Luo, Effect of holding time on the microstructure and mechanical properties of dual-phase steel during intercritical annealing, *J. Wuhan Univ. Technol. Mater. Sci. Ed.* **30** 156–161 (2015). <https://doi.org/10.1007/s11595-015-1118-5>.

- [2] M. Alibeyki, H. Mirzadeh, M. Najafi, Fine-grained dual phase steel via intercritical annealing of cold-rolled martensite, *Vacuum*. **155** 147–152 (2018). <https://doi.org/10.1016/j.vacuum.2018.06.003>.
- [3] Z. Xiong, K. Andrii, S. Nicole, V.P. Elena, Effect of Holding Temperature and Time on Ferrite Formation in Dual Phase Steel Produced by Strip Casting, *Mater. Forum*. **38** 44–48 (2014).
- [4] S. Wu, D. Wang, X. Di, C. Li, Z. Zhang, Z. Zhou, X. Liu, Strength-toughness improvement of martensite-austenite dual phase deposited metals after austenite reversed treatment with short holding time, *Mater. Sci. Eng. A*. **755** 57–65 (2019). <https://doi.org/10.1016/j.msea.2019.03.125>.
- [5] M. Zamani, H. Mirzadeh, M. Maleki, Enhancement of mechanical properties of low carbon dual phase steel via natural aging, *Mater. Sci. Eng. A*. **734** 178–183 (2018). <https://doi.org/10.1016/j.msea.2018.07.105>.
- [6] M. Aksoy, A. Esin, Improving the mechanical properties of structural carbon steel by dual-phase heat treatment, *J. Mater. Eng.* **10** 281–287 (1988). <https://doi.org/10.1007/BF02834157>.
- [7] X. Zuo, Y. Chen, M. Wang, Study on microstructures and work hardening behavior of ferrite-martensite dual-phase steels with high-content martensite, *Mater. Res.* **15** 915–921 (2012). <https://doi.org/10.1590/S1516-14392012005000118>.
- [8] Z. Xiong, A.G. Kostryzhev, Y. Zhao, E. V. Pereloma, Microstructure Evolution during the Production of Dual Phase and Transformation Induced Plasticity Steels Using Modified Strip Casting Simulated in The Laboratory, *Metals (Basel)*. **9** 449 (2019). <https://doi.org/10.3390/met9040449>.
- [9] Z.P. Xiong, A.G. Kostryzhev, N.E. Stanford, E. V. Pereloma, Microstructures and mechanical properties of dual phase steel produced by laboratory simulated strip casting, *Mater. Des.* **88** 537–549 (2015). <https://doi.org/10.1016/j.matdes.2015.09.031>.
- [10] E. Olorundaisi, T. Jamiru, T.A. Adegbola, O.F. Ogunbiyi, Modeling and optimization of operating parameters using RSM for mechanical behaviour of dual phase steels, *Mater. Res. Express*. **6** 105628 (2019). <https://doi.org/10.1088/2053-1591/ab430e>.
- [11] F.G. Caballero, A. García-Junceda, C. Capdevila, C.G. De Andrés, Evolution of microstructural banding during the manufacturing process of dual phase steels, *Mater. Trans.* **47** 2269–2276 (2006). <https://doi.org/10.2320/matertrans.47.2269>.
- [12] A.K. Panda, P.K. Ray, R.I. Ganguly, Effect of thermomechanical treatment parameters on mechanical properties of duplex ferrite-martensite structure in dual phase steel, *Mater. Sci. Technol.* **16** 648–656 (2000). <https://doi.org/10.1179/026708300101508225>.
- [13] K.K. Alaneme, C.M. Kamma, Phase transformation studies of a low alloy steel in the ( $\alpha + \gamma$ ) phase region, *Mater. Res.* **13** 113–117 (2010). <https://doi.org/10.1590/S1516-14392010000100022>.
- [14] W. Handoko, A. Anurag, F. Pahlevani, R. Hossain, K. Privat, V. Sahajwalla, Effect of selective-precipitations process on the corrosion resistance and hardness of dual-phase high-carbon steel, *Sci. Rep.* **9** 1–11 (2019). <https://doi.org/10.1038/s41598-019-52228-z>.
- [15] E. Salamci, S. Candan, F. Kabakci, Effect of microstructure on corrosion behavior of dual-phase steels, *Kov. Mater.* **55** 133–139 (2017). <https://doi.org/10.4149/km-2017-2-133>.
- [16] B.M. Gurumurthy, S.S. Sharma, A. Kini, Ferrite-Bainite Dual Phase Structure and Mechanical Characterization of AISI 4340 Steel, *Mater. Today Proc.* **5** 24907–24914 (2018). <https://doi.org/10.1016/j.matpr.2018.10.290>.

- [17] E. Olorundaisi, T. Jamiru, T.A. Adegbola, Mechanical and microstructural evaluation of dual phase steel, quenched in bitumen and water at an intercritical temperature: Effect of holding time, *Mater. Res. Express.* **6** 115606 (2019). <https://doi.org/10.1088/2053-1591/ab4747>.
- [18] F. Jamei, H. Mirzadeh, M. Zamani, Synergistic effects of holding time at intercritical annealing temperature and initial microstructure on the mechanical properties of dual phase steel, *Mater. Sci. Eng. A.* **750** 125–131 (2019). <https://doi.org/10.1016/j.msea.2019.02.052>.
- [19] K. Radwanski, R. Kuziak, R. Rozmus, Structure and mechanical properties of dual-phase steel following heat treatment simulations reproducing a continuous annealing line, *Arch. Civ. Mech. Eng.* **19** 453–468 (2019). <https://doi.org/10.1016/j.acme.2018.12.006>.
- [20] R.Y.P.A.S.C. Dhiraj Bhika Chaudhari, Effect of Quenching Parameters on Material Characteristics of Specimen- an Overview, *Int. J. Mech. Prod. Eng. Res. Dev.* **5** 25–32 (2015).
- [21] M.I. Ojovan, W.E. Lee, Immobilisation of Radioactive Waste in Bitumen, *An Introd. to Nucl. Waste Immobil.* 233–244 (2014). <https://doi.org/10.1016/b978-0-08-099392-8.00016-4>.
- [22] O. Emmanuel, O. Ikele, T. Jamiru, A. Adesola, J. Fayomi, B. Akhiwu, B. Akhiwu, Optimization and Microstructural Evaluation of Processing Parameters on the Density and Surface Hardness of Dual Phase Steel, *Sci. J. Res. Rev.* **3** 1–14 (2021). <https://doi.org/10.33552/sjrr.2021.03.000553>.
- [23] B.M. Gurumurthy, S. Shankar, A. Kini, Ferrite-Bainite Dual Phase Structure and Mechanical Characterization of AISI 4340 Steel, *Mater. Today Proc.* **5** 24907–24914 (2018). <https://doi.org/10.1016/j.matpr.2018.10.290>.
- [24] A.A. Adediran, Mechanical properties of dual phase steel quenched in bitumen medium Mechanical properties of dual phase steel quenched in bitumen medium, *Leonardo Electron. J. Pract. Technol.* 1–16 (2016). <https://doi.org/http://lejpt.academicdirect.org>.
- [25] M.O.H. AMUDA, E.T.A. T.A. OLANIYAN, L.O. OSOBA, Mechanical Properties of Bitumen Quenched Dual Phase Steel, *Sains Malaysiana.* **46** 743–753 (2017). <https://doi.org/http://dx.doi.org/10.17576/jsm-2017-4605-09>.